JOURNAL OF MATERIALS SCIENCE 8 (1973) 871–875

Cracking in yttrium orthoaluminate single crystals

B. COCKAYNE, B. LENT
Royal Radar Establishment, Malvern, Worcs, UK
J. S. ABELL, I. R. HARRIS
Department of Physical Metallurgy and Science of Materials, Birmingham University, UK

Several major factors which influence cracking in Czochralski-grown $YAlO_3$ single crystals have been identified. The procedures evolved for minimizing crack formation are also described.

1. Introduction

Single crystals of yttrium orthoaluminate ($YAlO_3$) doped with neodymium (Nd^{3+}) are a potential alternative to yttrium aluminium garnet as a solid state laser material. Crystals of $YAlO_3$ can be grown from the melt using the Czochralski technique, but a major difficulty encountered during growth and subsequent cutting of the crystals is a tendency to crack.

$YAlO_3$ is reported to have a perovskite-type orthorhombic crystal structure which can exhibit twinning and metastability [1, 2]. Hence, effects resulting from decomposition, anisotropic mechanical or thermal properties and twin formation, are possible intrinsic sources of cracking. Factors extrinsic to the material, such as crystal cooling rate and crystal size, are also likely to be important. This paper reports upon how these factors influence cracking and discusses methods by which cracking can be controlled.

2. Experimental details

The results described are based on an analysis of seventy Czochralski-grown crystals prepared in a substantially similar manner to sapphire single crystals [3]. The crystals were grown from melts contained in either 3.8 cm diameter × 3.3 cm deep or 5 cm diameter × 5 cm deep iridium crucibles. Stoichiometric melts were prepared from the component oxides; Y_2O_3 and Nd_2O_3 were supplied by Rare-Earth Chemicals Ltd whilst the Al_2O_3 was obtained from BDH Ltd. The respective crystal pull and rotation rates were 1 mm h^{-1} and 10 rev min^{-1}. Both inert (A/N_2) and slightly oxidizing ($A/N_2/O_2$) gas ambients were used to envelope the crystal and melt; the total gas flow rate was standardized at 0.5 l min^{-1}. Both *b*- and *c*-axis crystals were grown.

Mechanical properties were studied on rectangular-based prismatic crystal sections, 8 × 3 × 3 mm, cut with the compression axis, *a*, *b* or *c*, parallel to the long dimension. These specimens were located between alumina compression plates in a small Pt-40% Rh resistance wound furnace mounted on an Instron Universal Testing Machine. Dilatometric properties were recorded on similar specimens using apparatus described earlier [4].

3. General features of cracking

Two main types of cracking behaviour are evident in $YAlO_3$ single crystals, namely, surface cracking and bulk cracking. Surface cracks (Fig. 1a) are generally small, closely spaced and impart a translucent appearance to the crystal; they frequently appear to be generated from the seeding-on position. Bulk cracks (Fig. 1b) often follow crystallographic planes, especially at intersections with the crystal surface; cracks along both (001) and (010) planes have been identified.

4. General conditions governing crack formation

In a growth environment standardized with respect to crucible dimensions, melt volume and temperature gradients, in addition to the basic parameters such as pull rate, rotation rate etc.,

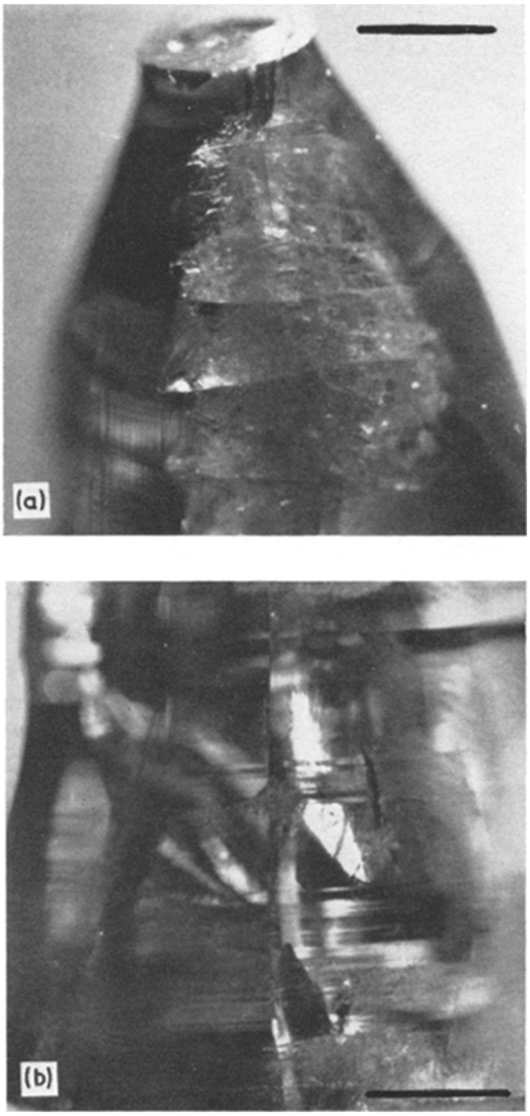

Figure 1 (a) Finely-spaced surface cracks adjacent to the seeding-on position (marker = 5 mm). (b) Bulk cracks along low index planes (marker = 5 mm).

cracking shows a major dependence upon crystal size, crystal orientation, the quality of the crystal surface and crystal seeding. There is a marked interplay between these factors so a specific dependence upon one particular factor is difficult to isolate. Even so, several important points have emerged as follows:

(i) large diameter crystals (18 to 20 mm) crack more readily than those of smaller diameter (10 to 12 mm);

(ii) *c*-axis crystals crack more readily than *b*-axis crystals (no *a*-axis crystals were grown);

(iii) rough-surfaced crystals grown in an inert atmosphere (A/N_2) crack more readily than the smooth surfaced crystals produced when 0.5 vol % O_2 is added to the gas ambient;

(iv) cracking which emanates from the seeding position is minimized by holding the seed in contact with the melt for a period of several hours prior to growth;

(v) crystals cooled at fast rates (1000° C h^{-1} to 100° C h^{-1}) tend to crack more readily than crystals cooled slowly (35° C h^{-1}) but the tendency is so often masked by the effects of (i) to (iv) that the cooling rate does not appear to be a major factor in controlling cracking during the growth cycle. However, crystals cooled at the faster rates frequently crack during subsequent machining operations;

(vi) cracking during the procedures used to shape the crystal into a laser rod can be almost eliminated by annealing the crystal subsequent to growth; a temperature of 1300° C and an annealing time of 12 h have been used since these conditions are consistent with the annealing procedure used to eliminate colour centres in $YAlO_3$ [5].

(vii) visual observations and optical pyrometric measurements of *c*-axis crystals whilst cooling have shown that cracking can occur at 1400 ± 50° C; crack initiation and propagation continues down to room temperature.

5. Crack-forming mechanisms

The ability of a material to withstand cracking depends principally upon its basic mechanical properties, the stresses to which it is subjected, intrinsic crystal defects and surface condition.

5.1. Hoop stresses and anisotropic contraction

The stresses to which a Czochralski-grown crystal is subjected are well documented [6]; the principal stress is a hoop stress, acting radially, which develops from differential thermal expansion induced because the crystal surface generally cools faster than the crystal centre. In *c*-axis $YAlO_3$ crystals, the hoop stress can exert maximum resolved shear stress on the predominant (110) twin planes [5] and, consequently, *c*-axis crystals twin readily. Twinning on one system of planes does not induce cracking (Fig. 2a), but when the conjugate system operates (Fig. 2b) cracking is commonly observed and appears to be nucleated from the twin intersections, where etch pit studies (Fig. 2c) reveal the high dislocation density typical of very strained regions of crystal. In *b*-axis crystals, the (1 1 0) twin planes are at 45° to the radial plane upon which the hoop stress exerts maximum influence. Consequently, the resolved stress on the twin plane is reduced which is consistent with the observed absence of twinning and associated cracking in *b*-axis crystals. The hoop stresses which develop in *c*-axis crystals could be accentuated by the difference in expansion behaviour, Fig. 3, determined for the *a*-, *b*- and *c*-axes. During cooling of *c*-axis crystals, anisotropic contraction will occur in the radial plane containing the directions along which the hoop stresses are a maximum, the plane being of the type *ab*. In the corresponding situation for *b*-axis crystals, the contraction will be approximately isotropic; the plane being of the type *ac*. In an isothermal environment the anisotropic contraction should be accommodated without inducing additional strain but, in the non-uniform temperature gradients experienced in Czochralski growth this contraction is likely to induce stresses which reinforce those arising from differential thermal expansion between the crystal centre and its periphery, and thereby, promote twinning and cracking in *c*-axis crystals.

The room temperature mechanical properties of $YAlO_3$, determined at a strain-rate of 10^{-4} sec^{-1}, confirm the differences in behaviour described for the crystal axes. When a compressive stress is applied along either the *a*- or *c*-axis, the specimens fail by brittle fracture at

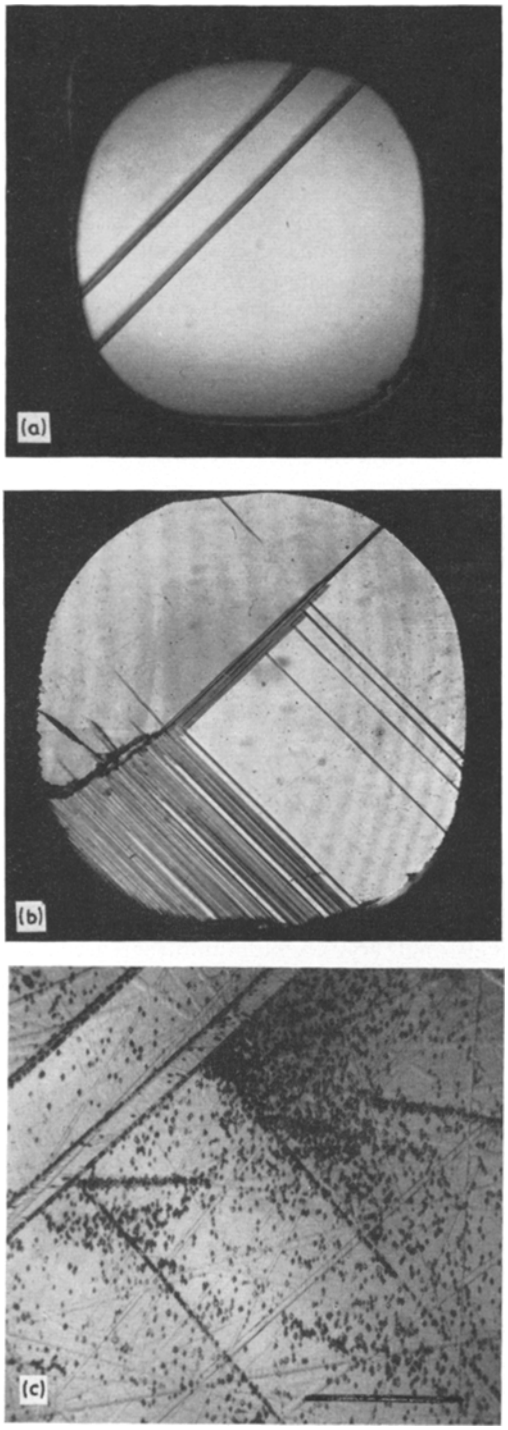

Figure 2 A transverse section of a [0 0 1]-axis crystal showing (a) twinning on one set of (1 1 0) planes (sample diameter = 14 mm), (b) conjugate twinning and crack nucleation (sample diameter = 13 mm), (c) a high dislocation density at twin intersections (marker = 1 mm).

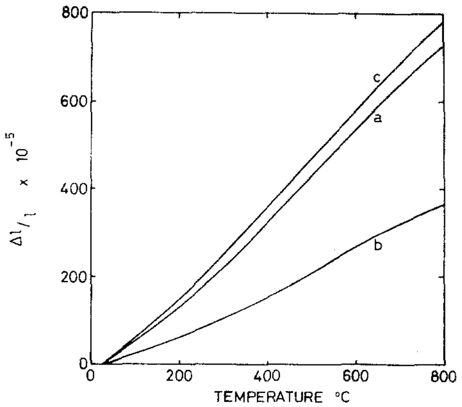

Figure 3 Expansion characteristics of the *a*-, *b*- and *c*-axes from *RT* to 800° C.

stress levels within the range 3500 to 9300 kg cm^{-2} with an absence of twinning prior to fracture. However, when a compressive stress is applied along the *b*-axis (equivalent to *c*-axis growth), twinning occurs on one set of (1 1 0) planes at the low stress of 500 kg cm^{-2}; this is rapidly followed by twinning on the conjugate system, the generation of microcracks at the twin intersections and failure. For comparison, the compressive fracture strength of $Y_3Al_5O_{12}$ under identical conditions was determined as 10000 kg cm^{-2}.

5.2. Surface condition

A scanning electron microscope examination of crystal surfaces has shown that the roughness associated with the inert gas ambient conditions is due to three features. These are shown in Fig. 4 and consist of regularly shaped particles (A), and grooves (B) some of which contain solidified material (C). In contrast, crystals grown in the presence of 0.5 vol % O_2 are smooth and featureless.

Electron probe X-ray microanalysis has shown that the particles are iridium. These can form either by vapour or melt transport from the crucible to the crystal. Vapour transport is the more likely possibility as melt transport usually causes a substantial number of iridium particles to be incorporated into the crystal, which is not the observed case. No compositional changes have been detected in the regions of B and C but both features are typical of surface etching effects induced by a slight loss of one or more components, in this case, presumably oxygen. This loss causes a localized reduction in melting point and the resulting liquid flows down the side of the crystal, thereby producing a groove akin to the solute trails sometimes observed within the bulk material. [7]. As it flows, this molten material dissolves the underlying matrix until it reaches the equilibrium melting point and solidifies within the groove. Defects A, B and C all impair the surface condition of the crystal and can act as local stress-raising points which enhance cracking.

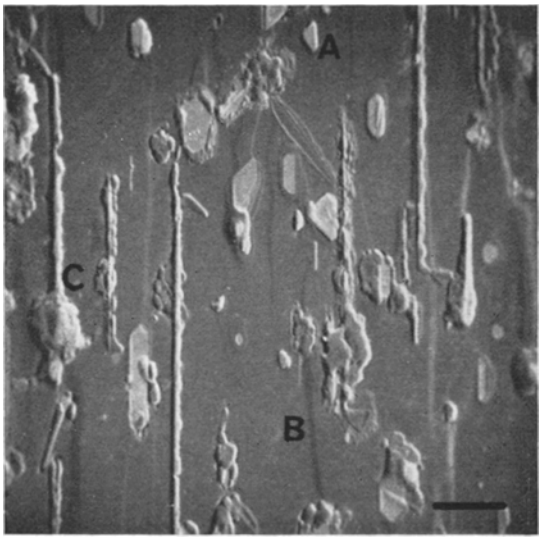

Figure 4 A scanning electron micrograph of the surface of a crystal grown in an inert atmosphere showing regularly shaped iridium particles (A) and trails typical of surface decomposition (B and C) (marker = 25 μm).

5.3. Crystal seeding

Strain can be induced at the seed/crystal interface either by lattice spacing differences between the seed and the crystal or by thermal shock. The second possibility seems most applicable to the present observations, as the prolonged soaking of the seed, which minimizes crack formation, is virtually an annealing process. Furthermore, lattice spacing differences should be negligible as seed and crystal had identical compositions.

5.4. Crystal defects

$YAlO_3$ single crystals exhibit many of the basic imperfections observed in Czochralski-grown oxide single crystals. Non-uniform segregation of added impurities, such as neodymium, is evident as growth striations and the formation of facets on the solid/liquid interface leads to an elastically strained central core within the crystal. These defects, illustrated in Fig. 5a, are very similar to those observed in crystals of $Y_3Al_5O_{12}$. However, although these defects undoubtedly raise the strain level of the crystal, no cracks have been observed emanating from such regions. Furthermore, nearly all the crack-free crystals grown contain both facets and striations.

A substantially more important defect is the presence of voids (Fig. 5b), which can occur in oxide crystals due to non-uniform segregation of gaseous impurities between solid and liquid. In $YAlO_3$ growth, these have occurred only at crystal pull rates greater than 3 mm h^{-1} but, when present, can nucleate both twins and cracks. Obviously, cracking from this source can be entirely eliminated by keeping the pull rate below the prescribed limit.

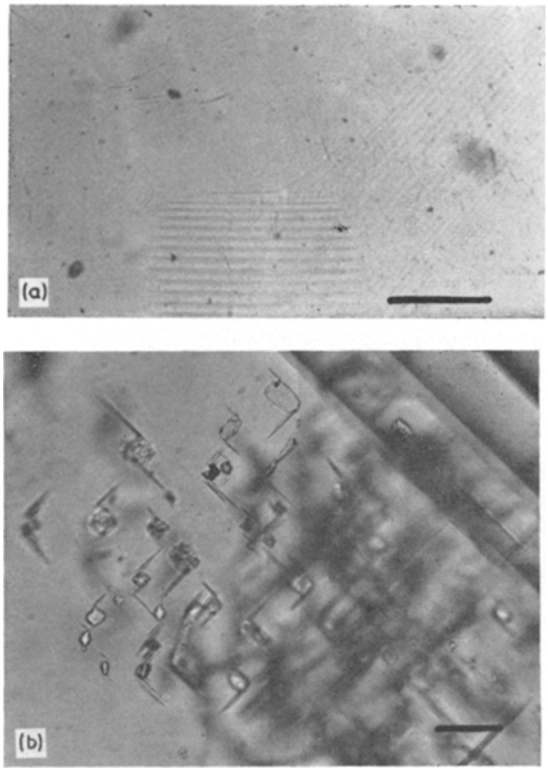

Figure 5 (a) Growth striations delineating the presence of a facet in a longitudinal section of a [001]-axis crystal containing 1 at. % Nd (marker = 200 μm). (b) Voids in a transverse section of a [001]-axis crystal (marker = 150 μm).

5.5. Metastability

There is no evidence to suggest that cracking can be attributed to metastability. Although $YAlO_3$ can be made to decompose in powder form [8], bulk specimens show neither visual nor X-ray evidence of structural change when annealed in the growth environment at temperatures up to 1800°C for periods of 160 h, a time and temperature span equivalent to a normal growth cycle.

6. Conclusions

Cracking is obviously a complex problem in $YAlO_3$. The predominant causes appear to be hoop stresses induced in the crystal during growth, defects in the crystal surface and thermal shock during seeding. A marked interplay occurs between these effects and subsidiary factors such as twinning mechanisms, anisotropic contraction, crystal diameter and crystal cooling rate. A number of defects such as facets and growth striations make little or no direct contribution to cracking.

The present work has established that the principal cracking mechanisms can be controlled. Nevertheless, the extent of cracking has important repercussions on the use of $YAlO_3/Nd^{3+}$ as a laser material because its mechanical properties during high temperature growth and room temperature compression are manifestly inferior to $Y_3Al_5O_{12}/Nd^{3+}$. Hence, although cracking can be minimized and high quality laser crystals produced, the relative mechanical instability of $YAlO_3$ may restrict its usefulness under the severe conditions experienced within a laser cavity and laser environments [9].

Acknowledgements

The authors wish to thank Dr A. W. Vere and K. H. Lloyd (RRE) for their respective assistance with the deformation studies and the scanning electron microscopy.

The paper is published by permission of the Copyright Controller, HMSO.

References

1. M. J. WEBER, M. BASS, K. ADRINGA, R. R. MONCHAMP, and E. COMPERCHIO, *Appl. Phys. Letts.* **15** (1969) 342.
2. I. WARSHAW and R. ROY, *J. Amer. Ceram. Soc.* **42** (1959) 434.
3. B. COCKAYNE, M. CHESSWAS, and D. B. GASSON, *J. Mater. Sci.* **2** (1967) 7.
4. A. W. VERE, J. G. PLANT, B. COCKAYNE, K. G. BARRACLOUGH, and I. R. HARRIS, *ibid* **4** (1969) 1075.
5. B. COCKAYNE and B. LENT, unpublished work.
6. D. T. J. HURLE, *Progr. Mater. Sci.* **10** (1962) 130.
7. B. COCKAYNE, *J. Crystal Growth* **3** (4) (1968) 60.
8. J. S. ABELL, I. R. HARRIS, and B. COCKAYNE, *J. Mater. Sci.* **7** (1972) 1088.
9. B. COCKAYNE, "Modern Oxide Materials" (Academic Press, London, 1972) p. 1.

Received 9 October and accepted 28 November 1972.